MODEL-BASED OPTIMAL OPERATION OF SEEDED BATCH CRYSTALLISATION PROCESSES

A. Mesbah[1, 2], J. Landlust[3], A.E.M. Huesman[1], H.J.M. Kramer[2], P.M.J. Van den Hof[1] and P.J. Jansens[2]
[1]Delft Center for Systems and Control, Delft University of Technology, the Netherlands.
[2]Process and Energy Laboratory, Delft University of Technology, the Netherlands.
[3]IPCOS BV, Boxtel, the Netherlands.
ali.mesbah@tudelft.nl

Dynamic optimization is applied for optimal control of a semi-industrial batch crystallisation process. The control strategy is based on a non-linear moment model. The dynamic model, consisting of differential and algebraic equations, is optimized using the simultaneous optimization approach in which all the state and input trajectories are parameterized. The resulting non-linear programming problem is then solved by a sequential quadratic programming algorithm. The optimal operation is realized by manipulation of the heat input to the crystallizer such that a maximum growth rate is maintained in the course of the process to avoid product quality degradation stemmed from irregular crystal growth. To be able to effectively track the maximum growth rate, the optimal heat input profile is computed on-line with feedback of process states estimated by an extended Luenberger-type observer; this enables the optimizer to reject the unmeasured process disturbances and also account for plant-model mismatch. Application of the on-line optimization strategy leads to substantial increase in the amount of crystals produced in a batch.

1. Introduction

Batch crystallisation processes are of paramount importance in the production of pharmaceuticals, food and speciality chemicals in the highly competitive chemical industry. Due to low-volume and high-value of such chemicals, interest in the optimal operation of batch crystallisation processes has substantially grown in the recent years. The principal operational challenge aims at increasing the productivity whilst satisfying product quality and batch reproducibility requirements.

The control of batch crystallisation processes is conventionally performed by manipulating the supersaturation trajectory due to its direct effect on the fundamental crystallisation phenomena, e.g. nucleation, growth, etc. There is a wealth of literature on improved operation of cooling batch crystallisation. These studies are, however, either based on the implementation of programmed cooling profiles [MAY88] that do not explore the use of dynamic optimization or are mainly concerned with open-loop implementation of off-line optimized cooling profiles [HU05] [NOW07]. The latter strategy, which has received considerable attention in the past decade in the light of the emergence of computationally powerful optimization tools and also more efficient dynamic optimization approaches, is not an effective optimal control strategy as open-loop implementation often deteriorates the performance of off-line optimized profiles.

In order to effectively cope with the inherent shortcomings of the open-loop optimal control due to plant-model mismatch, unmeasured process disturbances, irreproducible start-up and lack of reliable measurements for system states, the optimal operating policy can be computed on-line, the so-called closed-loop optimal control. Contrary to the open-loop optimal control, there are only few studies on closed-loop optimal control reported in the literature [ZHA03] [SHI06]. In these studies, a model-based optimization strategy in conjunction with a state estimator, also known as observer, is utilized to compute the optimal operating policy in a feedback control configuration where the effects of plant-model mismatch and unmeasured process disturbances are accounted for by continuous state

adaptation. Neither of the aforementioned studies, however, shows the viability of real-time dynamic optimization of batch crystallisation processes experimentally as they are only concerned with simulations of optimal control profiles applied to cooling crystallisation processes.
Recently, Mesbah et al. [MES08] devised a model-based feedback control system on the basis of a sequential dynamic optimizer in combination with an extended Luenberger-type observer and experimentally demonstrated its feasibility for real-time applications. Sequel to the preceding work, this study concerns the development of a simultaneous dynamic optimizer which is embedded in a similar model-based feedback control system. The performance of the optimal control strategy is examined by a number of open-loop and closed-loop implementations on a semi-industrial fed-batch evaporative crystallizer. It is worth noting that the major advantage of the simultaneous optimization approach is its superior computational efficiency as opposed to the sequential optimization approach.
The paper is organised as follows. In Section 2, the seeded fed-batch evaporative crystallisation process at hand is described and a process model for an ammonium sulphate-water system is presented. Section 3 includes description of the feedback control structure, as well as the formulation of the dynamic optimization problem. Section 4 discusses the experimental implementation of the proposed control strategy, followed by the concluding remarks given in Section 5.

2. Process description and modelling

The fed-batch evaporative crystallisation of the ammonium sulphate-water system is performed in a 75-liter draft tube crystallizer. The crystallizer can be considered as a single perfectly-mixed compartment with one inlet and two outlet streams. The crystal-free feed stream containing ammonium sulphate solution saturated at 50°C serves as the inlet flow to keep the crystallizer volume constant by compensating for losses in volume due to evaporation of solvent, i.e. water, and the slurry sampling. The vapour stream, free from crystal and solute, as well as an unclassified product removal stream comprise the outlet flows. The small product flow is withdrawn from the crystallizer at regular time intervals and diluted with saturated feed solution for on-line measurement of the Crystal Size Distribution (CSD) with a laser diffraction instrument (HELOS-Vario, Sympatec, Germany). The crystallisation is carried out isothermally at 50°C.
In order to ensure the reproducibility of batches, as well as the achievement of desired product specifications, seeded experiments are done. Ground seeds are prepared by milling and sieving of commercial product crystals of ammonium sulphate (DSM, The Netherlands) to collect 0.6 kg of the sieve fraction of 90-125 µm. The seed crystals are aged for one hour in a saturated solution of ammonium sulphate in a seeding vessel at 50°C prior to insertion into the crystallizer [KAL07]. An in-line concentration measuring probe (LiquiSonic®, SensoTech, Germany) is utilized to measure the predetermined supersaturation level at which the ground seeds are introduced.
The dynamic behaviour of a crystallisation process is typically captured by a Population Balance Equation (PBE) along with mass and energy balance equations. Under the assumptions of perfectly-mixed suspension, constant crystallizer volume, nucleation of crystals of infinitesimal size, negligible breakage and agglomeration and size-independent growth of crystals, the PBE for the fed-batch process at hand is expressed as follows:

$$\frac{\partial n(t,L)}{\partial t} = -G\frac{\partial n(t,L)}{\partial L} - \frac{F_p}{V}n(t,L) \tag{1}$$

with the following initial and boundary conditions:

$$n(0,L) = n_0(L) \tag{2}$$

$$n(t,0)=\frac{B_0}{G} \tag{3}$$

where n is the number density (#.m^{-3}.m^{-1}), G is the crystal growth rate (m.s^{-1}), B_0 is the total rate of nucleation (#.m^{-3}.s^{-1}), L is the characteristic length of crystal (m), V is the crystallizer volume (m^3) and F_p is the unclassified product removal flow rate (m^3.s^{-1}).

The method of moments [RAN71] is applied to Eq. (1) in order to reformulate the PBE into a set of computationally affordable reduced-order Ordinary Differentially Equations (ODEs). Upon multiplying both sides of Eq. 1 by $L^i dL$ and integrating over the entire crystal size domain, the following set of ODEs that describes the evolution of moments of CSD in time is obtained:

$$\frac{dm_i}{dt}=0^i\cdot B_0+i\cdot Gm_{i-1}-\frac{m_i F_p}{V} \qquad \mathrm{i}=0,...,4 \qquad \mathrm{m_i}(0)=m_{i,0} \tag{4}$$

Due to the isothermal operation of the crystallizer, the mass and energy balance equations simplify to a single expression for the solute concentration:

$$\frac{dC}{dt}=\frac{F_p\left(C^*-C\right)\!/V+3K_V Gm_2\left(k_1+C\right)}{1-K_v m_3}+\frac{k_2 Q}{1-K_V m_3} \qquad \mathrm{C}(0)=C_0 \tag{5}$$

where Q is the heat input to the crystallizer (kW), K_V is the crystal volumetric shape factor, C^* is the equilibrium concentration (kg $_{\text{solute}}$/kg $_{\text{solvent}}$) and the constant coefficients k_1 and k_2 are given by:

$$k_1=\frac{H_v C^*}{H_v-H_L}\left(\frac{\rho_c}{\rho_L}-1+\frac{\rho_L H_L-\rho_c H_c}{\rho_L H_v}\right)-\frac{\rho_c}{\rho_L} \quad \text{and} \quad k_2=\frac{C^*}{V\rho_L\left(H_v-H_L\right)} \tag{6}$$

In addition to the first five moments of the CSD and the solute concentration balance, power law empirical expressions are used to describe the crystallisation phenomena, namely the total nucleation rate B_0 and the size-independent crystal growth rate G:

$$B_0=k_b m_3 G \tag{7}$$

$$G=k_g\left(C-C^*\right)^g \tag{8}$$

The physical properties of the ammonium sulphate-water system, as well as the nucleation and growth rate kinetic parameters are listed in Table 1.

It follows from the abovementioned analysis that the dynamics of the system under investigation is governed by a set of Differential Algebraic Equations (DAEs), i.e. equations (4)-(8). The choice of the moment model in this study can be motivated from two perspectives. Firstly, the supersaturation level is relatively low in batch runs due to large seed loadings at the beginning of each batch run [DOK02]. This phenomenon leads to minimization of secondary nucleation and, therefore, crystal growth is mainly responsible for the evolution of CSD throughout the batch run. Secondly, numerical solution of the full PBE often requires considerable computational effort which might render the real-time implementation of the model-based control strategy infeasible.

Table 1. Model parameters

Symbol	Parameter	Value	Unit
C^*	Saturation concentration	0.46	kg $_{solute}$/kg $_{solution}$
g	Growth rate exponent	1	-
H_c	Specific enthalpy of crystals	60.75	kJ/kg
H_L	Specific enthalpy of liquid	69.86	kJ/kg
H_V	Specific enthalpy of vapor	2.59×10^{3}	kJ/kg
K_V	Volumetric shape factor	0.43	-
k_b	Nucleation rate constant	1.02×10^{14}	#/m^4
k_g	Growth rate constant	7.50×10^{-5}	m/s
F_p	Product flow rate	1.73×10^{-6}	m^3/s
V	Crystallizer volume	7.50×10^{-2}	m^3
ρ_c	Density of crystals	1767.35	kg/m^3
ρ_L	Density of saturated solution	1248.93	kg/m^3

3. On-line dynamic optimization

In batch crystallisation processes, fulfilment of the desired requirements of the final product quality is often of greater significance than maximization of process yield or energy saving considerations. Hence, crystal growth dominant operation is more desirable than nucleation dominant operation since the latter phenomenon adversely influences the product quality. Crystal dominant operation may, however, require long batch times to attain the required product specifications in terms of crystal size, as well as fairly high batch crystal yield due to low supersaturation levels during the batch. This implies that the optimal control problem should be formulated such that a compromise between a reasonably fast growth rate and a low nucleation rate is sought by manipulating the supersaturation level in the course of the batch run.

This study aims at improvement of the product quality by controlling the crystal growth rate as excessive growth rates often result in quality degradation, namely irregular crystal habits, impurity uptake, liquid inclusions etc. This objective is realized by formulating a dynamic optimization problem as follows:

$$\begin{aligned} \min_{Q_{in}(t)} \quad & \int_0^{t_f} \left(100\frac{G(t)-G_{max}}{G_{max}} \right)^2 dt \Big/ \int_0^{t_f} \mathrm{d}t \\ s.t. \quad & \text{equations (4) - (8)} \\ & Q_{low} \le Q(t) \le Q_{high} \end{aligned} \tag{9}$$

where Q is the heat input profile parameterized using a piecewise-constant function of time with equidistant time intervals, t_f is the batch time and G_{max} is an arbitrarily chosen maximum crystal growth rate to avoid the formation of irregularly shaped crystals and limit the undesirable effect of nucleation ($G_{max} = 2.5\times10^{-8}\ \mathrm{m.s^{-1}}$). An inequality constraint is imposed on the heat input; the lower limit Q_{low} is to ensure the survival of ground seeds during the initial phase of the batch, whereas the upper actuator constraint Q_{high} is due to physical limitations of the process. It is worth noting that the optimal control problem expressed in Eq. (9) indicates the desire to sustain the product quality during the batch run while the maximization of batch crystal yield is also sought as the secondary interest.

The abovementioned optimization problem is solved in GAMS simulation environment using CONOPT3 solver which is well suited for solution of constrained optimization problems by means of Non-Linear Programming (NLP) algorithms. The optimal control problem is thereby

converted to an NLP problem via simultaneous optimization approach [HUE07] in which all the differential equations are transformed to algebraic equations by parameterization of state and input trajectories. The implicit Euler scheme is utilized for discretization of all variables due to its unconditional stability. The input and state profiles consist of 180 elements spanned over a prediction horizon of 3600 s.

The feedback control strategy depicted in Figure 1 is devised to employ the dynamic optimizer for real-time implementations. In this framework, the dynamic optimization problem is continually solved on-line in a receding horizon mode such that the deviations of the process output, i.e. crystal growth rate, from the reference trajectory, i.e. G_{max}, are kept as small as possible in the presence of plant-model mismatch and unmeasured disturbances. Thus, an observer is utilized to estimate the initial conditions x_{est} required to initialize the optimization problem recursively at regular time intervals based on the process model and available process measurements y_{meas}. The observer also enables to estimate the supersaturation profile, i.e. solute concentration, for which actual measurements are not obtainable. In this study, the extended Luenberger-type observer designed on the basis of the moment model [KAL06] is used to reinitialize the dynamic optimizer every 120 s, when new information on system states is made available through CSD and crystal content measurements. Then every 20 s, the first element of the optimal operating policy, i.e. heat input profile, is taken as the set-point value and applied to the process using a conventional PI controller which takes a control action u to eliminate the difference between the process value of heat input Q_{pv} and the set-point Q_{sp}. The PI controller is embedded in a Distributed Control System (DCS, CENTRUM CS3000, Yokogawa, Japan) that forms the basic control layer. An OPC (**O**LE (Object Linking and Embedding) for **P**rocess **C**ontrol) server (IPCOS, The Netherlands) enables the timed signal exchange among various modules of the control architecture.

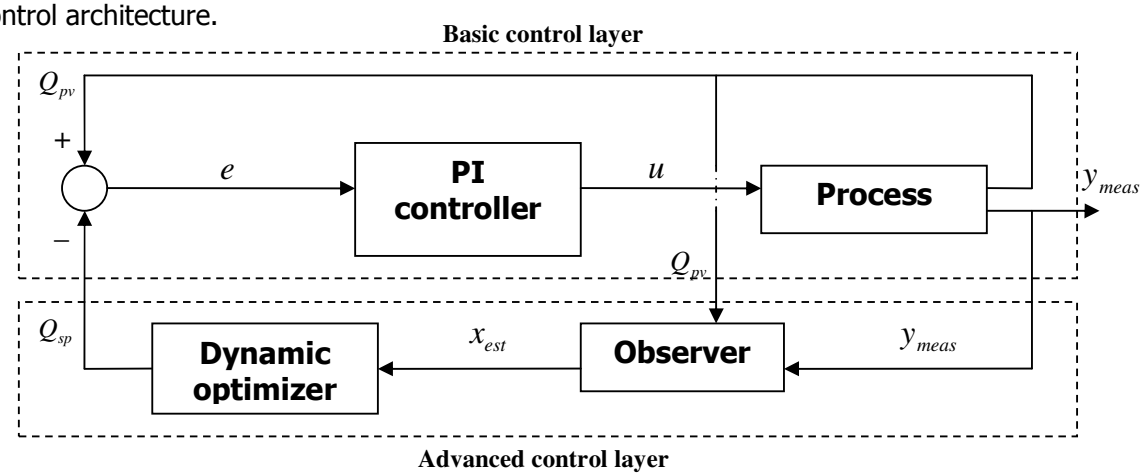

Figure 1. Block diagram of the on-line optimal control system.

4. Experimental implementation

The performance of the proposed control structure is experimentally evaluated by a number of real-time implementations on the 75-liter draft tube crystallizer described in Section 2. Since in seeded batch runs the crystal growth rate predominantly determines the product quality [KAL07], the variations of growth rate in relation to different heat input profiles are investigated in this study.

The first three experiments aim at revealing the need for effective crystal growth rate control and determination of the effectiveness of on-line computation of the optimal control profile as opposed to open-loop implementation of the off-line optimized profile. Figures 2 and 3

depict the heat input and growth rate profiles, respectively. As shown, when the heat input to the crystallizer is kept constant at 9 kW throughout experiment DT_c31, the growth rate does not fulfil the crystal growth rate constraint, represented by the dashed line in Figure 3, and steadily descents. This implies that a control action has to be taken in order to meet the growth rate constraint. The optimal operating policy is, therefore, computed off-line and manually applied to the process as a time-varying set-point of the heat input PI controller during experiment DT_c55. Figure 3 however shows that the growth rate is yet again unable to closely track the constraint as a result of open-loop implementation of the optimal heat input trajectory.

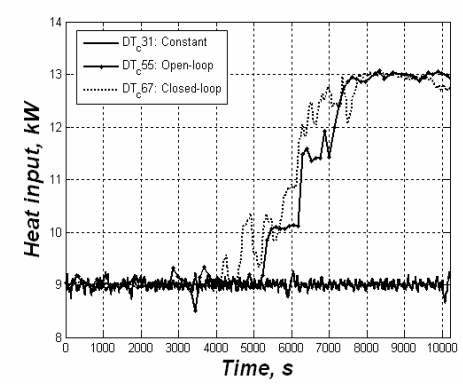

Figure 2. Heat input profiles.

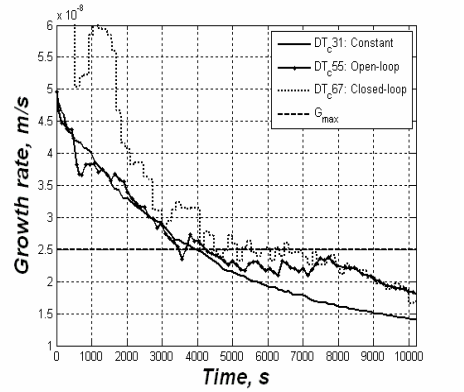

Figure 3. Crystal growth rate profiles.

The deficiency in fulfilling the growth rate constraint stemmed from open-loop implementation of the optimal operating policy motivates the on-line computation of the optimal heat input trajectory in experiment DT_c67. As depicted in Figure 3, when the growth rate crosses the constraint after 4000 s, it is forced to follow the maximum growth rate by raising the heat input to the crystallizer. The constraint cannot however be tracked any longer as soon as the heat input reaches its upper bound of 13 kW and, consequently, the growth rate gradually drops while the heat input remains at its maximum admissible value. It is evident that the closed-loop implementation of the dynamic optimizer offers a better constraint tracking till actuation limitation renders the optimal control of the batch process impossible. This superior performance is due to the feedback structure and the receding horizon implementation of the control system that account for plant-model mismatch and enable disturbance handling by state adaptation in the observer.

Figure 3 exhibits that the growth rate constraint is not maintained in the initial phase of the batch since the heat input cannot be lowered below 9 kW. This is due to its hard constraint to suppress possible dissolution of the inserted seeds as has been suggested by [KAL06]. To investigate the effect of this constraint on the product quality, i.e. crystal size, and to attain a more effective optimal control of the crystal growth rate, the lower bound of heat input in Eq. 9 is lessened to 3.0 kW. The heat input and growth rate profiles corresponding to the closed-loop implementation of the dynamic optimizer subjected to the new constraint are displayed in Figure 4 and Figure 5, respectively. In experiment DT_c69, the seeds are introduced into the crystallizer at heat input of 9 kW; then having obtained 5 reliable CSD measurements to appropriately initialize the dynamic optimizer, the optimal control system is switched on. Figure 5 shows that a control action is immediately taken to bring the growth rate to its constraint by decreasing the heat input to 3.7 kW. Subsequently, a fairly well growth rate constraint tracking is achieved till the heat input reaches its maximum admissible value, i.e. 13 kW. The effectiveness of applying an on-line optimal control strategy to maintain the maximum crystal growth rate in the course of a batch crystallisation process can be clearly inferred from Figure 5 that shows an uncontrolled process, i.e. experiment DT_c70, would lead to continual violation of the maximum growth rate.

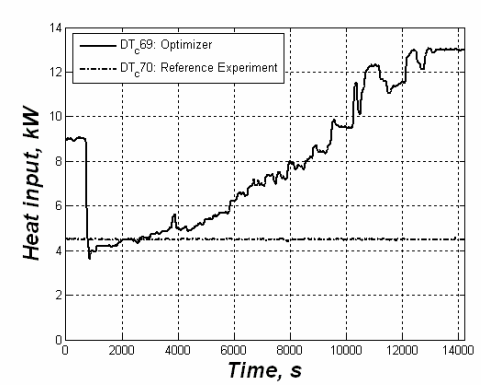

Figure 4. Optimal heat input profile for the entire batch time.

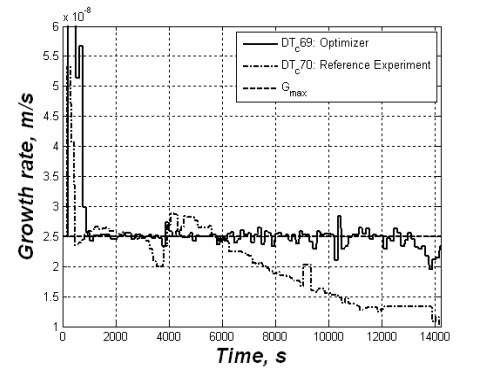

Figure 5. Optimal crystal growth rate profile for the entire batch time.

Figure 6 reveals that higher growth rates obtained in batch DT_c69 result in a 60% increase in the batch yield as compared to experiment DT_c70 with constant heat input profile of 4.5 kW, whereas the crystals are also slightly larger; see Figure 7. It is evident from Figure 6 that lowering the heat input constraint rather substantially reduces the amount of crystals produced in a batch. The spikes in Figure 6 are due to sweep of the product line of the crystallizer with rinsed water to avoid plugging.

The evolution of median crystal size during different batches is depicted in Figure 7. As can be seen, the crystals in the first CSD measurement sample taken after insertion of the seeds at heat input of 4.5 kW are about the same size of the crystals when seeds are inserted at 9 kW, owing to the optimal seeding procedure that circumvents irreproducible start-ups due to uncertain initial conditions. The seeds thereby do not dissolve when they are exposed to heat input of 4.5 kW. Figure 7 also shows that the crystal size achieved at the batch end, i.e. 12000 s, in experiment DT_c67 is almost identical to that of the batch DT_c69. This suggests that lowering the heat input constraint would not affect the product quality in terms of crystal size. Nonetheless, the impact of effective control of the growth rate in the initial phase of a batch on the product quality in terms of crystal habit is yet to be investigated.

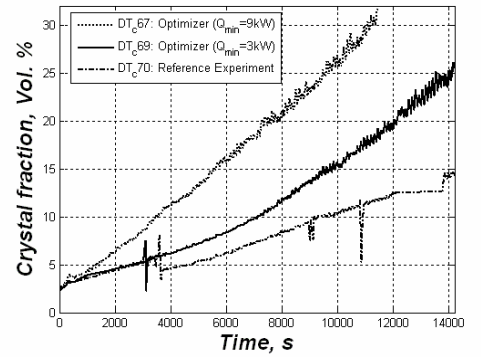

Figure 6. Batch crystal yield.

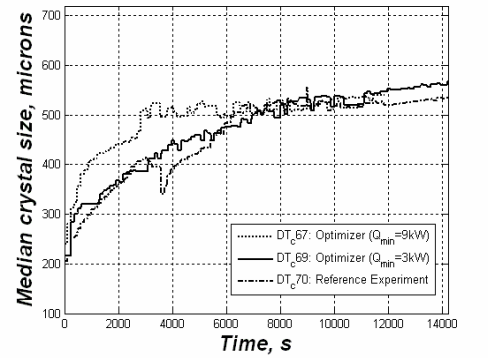

Figure 7. Median crystal size.

5. Conclusions

In this paper a dynamic optimization strategy for industrial batch crystallization processes is developed and experimentally validated on a 75-liter evaporative draft tube crystallizer. It is revealed that dynamic optimization is an effective control strategy for model-based optimal operation of batch crystallizers. The results also indicate that deliberate choice of the optimization approach can make real-time implementations of a model-based control strategy feasible.

It is shown that open-loop implementation deteriorates the effectiveness of optimal profiles due to plant-model mismatch and unmeasured disturbances. Such shortcomings can however be accounted for by on-line computation of the optimal trajectories with feedback of the estimated process states to the dynamic optimizer. Furthermore, the constraints to which the optimal control problem are subjected may considerably restrict the optimal operation of the process. As demonstrated, relaxing the heat input constraint leads to far better control of the crystal growth rate that in turn determines the product quality.
In future, the current work will be extended to optimal control of an 1100-liter draft tube baffle crystallizer equipped with a fines removal loop that offers an extra degree of freedom to better control the CSD. The choice of the simultaneous dynamic optimization will become more attractive as it would probably render the use of a full PBE model computationally affordable for real-time applications of a model-based optimal control strategy.

6. References

[DOK02] Doki, N., Kubota, N., Yokota, M., Chianese, A., Determination of critical seed loading ratio for the production of crystals of uni-modal size distribution in batch cooling crystallisation of potassium alum, J. Chem. Eng. Japan 35 (2002), 670-676

[HU05] Hu, Q., Rohani, S., Wang, D.X., Jutan, A., Optimal control of a batch cooling seeded crystallizer, Powder Technology 156 (2005), 170-176

[HUE07] Huesman, A.E.M., Bosgra, O.H., Van den Hof, P.M.J., Degrees of freedom analysis of economic dynamic optimal plantwide operation, 8th International IFAC Symposium on Dynamics and Control of Process Systems, Cancun Mexico, June 2007

[KAL06] Kalbasenka, A.N., Landlust, J., Huesman, A.E.M., Kramer, H.J.M., Application of observation techniques in a model predictive control framework of fed-batch crystallisation of ammonium sulphate, WCPT-5, Orlando Florida, April 2006

[KAL07] Kalbasenka, A.N., Spierings, L., Huesman, A.E.M., Kramer, H.J.M., Application of seeding as a process actuator in a model predictive control framework for fed-batch crystallisation of ammonium sulphate, Part. Part. Syst. Charact. 24 (2007)1, 40-48

[MAY88] Mayrhofer, B., Nyvlt, J., Programmed cooling of batch crystallizers, Chem. Eng. Process 24 (1988), 217-220

[MES08] Mesbah, A., Kalbasenka, A.N., Huesman, A.E.M., Kramer, H.J.M., Van den Hof, P.M.J., Real-time dynamic optimization of batch crystallisation processes, IFAC08, Seoul South Korea, July 2008

[NOW07] Nowee, S.M., Abbas, A., Romagnoli, J.A., Optimization in seeded cooling crystallization: A parameter estimation and dynamic optimization study, Chem. Eng. Process 46 (2007), 1096-1106

[RAN71] Randolph, A, Larson, M, Theory of Particulate Processes, Academic Press, 1971

[SHI06] Shi, D., El-Farra, N.H., Li, M., Mhaskar, P., Christofides, P.D., Predictive control of particle size distribution in particulate processes, Chem. Eng. Sci. 61 (2006) 268-281

[ZHA03] Zhang, G.P., Rohani, S., On-line optimal control of a seeded batch cooling crystallizer, Chem. Eng. Sci. 58 (2003), 1887-1896